

A Method of Terrain Crack Removal Suited for Large Differences in Boundary LoD

Chengming Li, Zhendong Liu and Xiaoli Liu
Chinese Academy of Surveying and Mapping, Beijing, China

Keywords: Terrain Cracks, Boundary LoD Level, Elevation Adjustment, Quadtree Data Structure, Terrain Crack Removal, Lighting Continuity.

Abstract: Terrain crack removal is an unavoidable problem that must be solved in real-time three-dimensional (3D) terrain rendering. Conventional elevation adjustment-based crack removal methods are plagued by a number of problems, including restrictions associated with level of detail (LoD) differences, computational inefficiency and lighting discontinuities. To address these issues, we propose a crack elimination method that is suited for large differences in boundary LoD. The first step in this method is the construction of terrain quadtrees that contain edge and angle adjacency information. These structures are then updated in real time. The second step is to modify the boundary mesh vertices using linear interpolation, which allows for LoD differences greater than 1 between adjacent tiles. Finally, the vertex normals of the mesh vertices of the terrain block are calculated and evaluated. Our method was experimentally validated using topographical data from a mountainous region in Sichuan Province, and the results provide evidence that supports the reliability and superiority of the proposed method compared to the conventional method.

1 INTRODUCTION

The occurrence of terrain cracks in the level of detail (LoD) rendering technique is caused by inherent differences in the LoD. When two adjacent terrain meshes have different LoDs, the elevations of their boundary grids will not be fully consistent, which causes the appearance of gaps in real-time terrain rendering processes (Yin et al, 2006). Currently, the most common method of terrain data simplification (both in China and abroad) is view-dependent continuous LoD rendering (Bulatov et al, 2013), which entails the use of view-dependent LoDs in terrain representations. Therefore, the elimination of terrain cracks is an unavoidable problem that must be solved in real-time three-dimensional (3D) rendering processes.

The most common methods of terrain crack removal are the adjustment of mesh boundary vertices (Han et al, 2008), patching methods (Li et al, 2013, Wan et al, 2015) and template decomposition (Xu et al, 2005, Wang et al, 2007). Since the adjustment of mesh boundary vertices does not require the creation of additional meshes, these methods are well suited for the representation of complex 3D terrain. Zhao et al. (2012) investigated a method for the seamless

expression of global multiresolution digital elevation models (DEMs) based on spherical degenerate quadtree grids. They designed an adaptive algorithm that seamlessly stitches cracks within and between quadtree blocks. The underlying mechanism of this algorithm involves merging the nodes of terrain blocks that have low LoDs among adjacent terrain blocks (Zhao et al, 2012). However, the aforementioned methods require the terrain to be completely retraversed and the relevant nodes to be retriangulated, which eliminates the independence of these nodes (Liu et al, 2010). These methods may also disrupt the rules that are normally used to control the terrain LoD (Zhao et al, 2002). To address these issues, we have proposed a method of terrain crack removal that can handle large differences in boundary LoD based on analyses of quadtree data structures and the rules for controlling the LoD.

The remaining sections of this paper are organized as follows. The second section describes the current method of adjusting mesh boundary vertices and the inadequacies of this method. The third section provides a detailed description of the improved crack removal method proposed in this paper. The experimental validation of this method is presented in Section 4. The fifth section provides a discussion of the method and the conclusions of the study.

2 RELATED WORK

2.1 Current Method of Adjusting Mesh Boundary Vertices

Methods for adjusting mesh boundary vertices are being continuously developed and refined by researchers around the world. Notably, Zhao et al. (2002) proposed a crack removal method based on the adjustment of elevation values. A basic description of this method is given as follows.

The method of Zhao et al. uses a hierarchical segmentation algorithm that eliminates cracks by instituting dependencies between vertices. When this method is used, the addition of a vertex will affect the parent node and adjacent node. Hence, vertex selection/elimination and mesh generation must be performed separately, and the independent rendering of each terrain block is difficult in this method. Since triangulation is not used in this method, operations such as the splitting of high-LoD meshes or the merging of low-LoD meshes cannot be performed, and this limitation disrupts the structure of the terrain mesh and eliminates node independence. The seamless stitching of terrain blocks is achieved by altering the elevation values of the vertices that are responsible for inducing cracks. Fig. 1(a) is an example of terrain cracks. In this case, adjustments will be made to the boundary vertices that belong to the node that has a higher level of resolution. In Fig. 1(b), the elevations of the A and B vertices (which belong to the upper left node) have been recalculated and reevaluated according to the boundary vertices of the adjacent node.

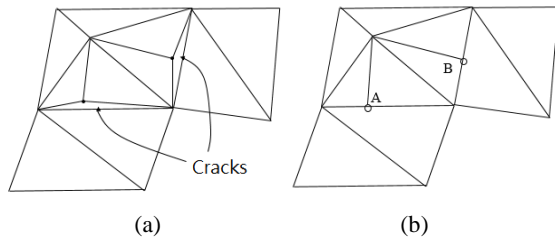


Figure 1: Crack elimination via the adjustment of elevation values: (a) Crack generation and (b) T-joints.

2.2 Inadequacies of the Current Method

Elevation adjustment-based crack elimination algorithms can be used to remove cracks by adjusting the elevation of mesh boundary vertices without

requiring triangulation. However, certain aspects of these algorithms remain problematic.

(1) Cracks can be generated by adjacent nodes with LoDs that are different by more than 1, but this scenario is not accounted for in current elevation adjustment-based crack removal algorithms. Furthermore, this scenario is likely to occur in complex terrain areas during real-time 3D terrain rendering.

(2) During crack removal, real-time CPU calculations are required to traverse the entirety of the terrain. This process is a highly time consuming when massive terrain data are involved.

(3) After the vertex elevations around the cracks have been adjusted by these algorithms, certain discontinuities will become apparent in the lighting of the terrain. In Fig. 2, for instance, the right side of boundary vertex A (terrain block 1) is not included in any triangular mesh. The right side of vertex A will therefore be excluded during the calculation of vertex normals, which subsequently leads to discontinuities between the vertex normal of A and the adjacent vertices. This issue will subsequently affect the terrain lighting calculations in 3D scenes and lead to errors in illumination-based terrain analyses.

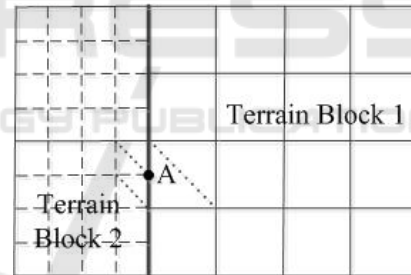


Figure 2: Lighting calculation for a pair of terrain blocks.

3 IMPROVED TERRAIN CRACK REMOVAL METHOD

The crack removal method we have proposed is suitable for large boundary LoD differences and consists of three primary steps: (1) the construction of terrain quadtree structures that contain edge and angle adjacency information and an algorithm for real-time updates, (2) the elimination of cracks caused by large differences in LoD, and (3) the calculation and updating of the vertex normals of terrain blocks.

3.1 The Construction of a Quadtree Structure That Contains Adjacency Information and the Dynamic Updating of This Structure

Differences in the rendering precision of adjacent terrain nodes are the root cause of terrain cracks (Fu et al, 2012. WIESEMANN et al, 2005). Therefore, the key to eliminating terrain cracks is the accurate recognition and determination of terrain node adjacencies when real-time LoD terrain rendering is implemented based on quadtree features. The following definitions have been provided to facilitate the description of the algorithm.

(1) Terrain nodes, such as A1 and A2 in Fig. 3, are simply referred to as tiles. A unified code is used to describe the LoD, row and column of each tile, i.e., Tilecode = (LoD, TileX, TileY). Each tile contains M×M vertices, with M being a positive integer that represents the number of grid points on a given edge.

(2) In a terrain quadtree, "parentless" nodes, such as C1 in Fig. 3, are referred to as root nodes, and "childless" nodes, such as C2, C6 and C7 in Fig. 3, are referred to as leaf nodes.

(3) The tiles that surround each tile are categorized either as edge neighbors or corner neighbors based on their spatial relationships. Edge neighbors can be classified as left edge neighbors (LN), upper edge neighbors (UN), right edge neighbors (RN), and bottom edge neighbors (DN). Corner neighbors may be classified as left upper corner neighbors (LUN), right upper corner neighbors (RUN), right lower corner neighbors (RDN), and lower bottom edge neighbors (LDN). An example of these spatial relationships is illustrated in Fig. 4.

(4) In a quadtree structure, "child" nodes on the upper left, upper right, bottom right and bottom left corners of a "parent" node are referred to as LUCHild, RUCHild, RDChild and LDChild, respectively.

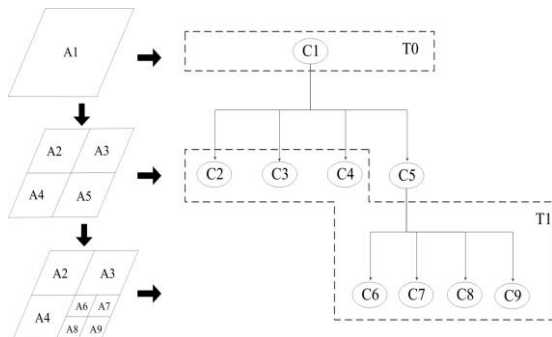


Figure 3: Terrain quadtree structure.

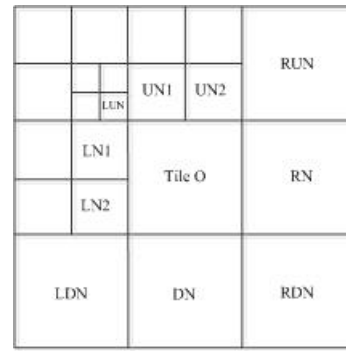


Figure 4: Definitions of adjacency relationships.

3.2 The Construction and Dynamic Updating of Quadtree Structures

During the rendering of a 3D terrain scene, terrain quadtrees will be constructed and dynamically updated according to the rules of view-dependent LoD control (Feng et al, 2010. Lindstrom et al, 2001). A change in view will therefore affect the merging and splitting of leaf nodes in a quadtree. For instance, Fig. 5(a) describes a terrain quadtree that corresponds to the view being close to the upper-left part of the terrain, and Fig. 5(b) illustrates the changes in the quadtree when the view shifts from the upper-left part of the terrain to the bottom-left part. When the quadtree changes from Fig. 5(a) to Fig. 5(b), the LDChild1 tile in Fig. 5(b) will split into four "children" tiles, and the LUCHild2, RUCHild2, RDChild2 and LDChild2 tiles in Fig. 5(a) will be merged. This process corresponds to the rendering of the "parent" tile (LUChild1).

The dynamic updating of adjacency information associated with the generation of "children" tiles or the merging of "parent" tiles (when the "parent" tile is being rendered) is a crucial step in crack removal. This adjacency processing algorithm can be divided into two modules according to the intrinsic characteristics of each leaf node: an algorithm that processes the adjacency information of split leaf nodes, and an algorithm that processes the adjacency information of merged leaf nodes.

Since terrain cracks only occur at inter-tile boundaries, the ultimate purpose of crack removal is to ensure that the four edges and corners of a tile are consistent with those of adjacent tiles. The assessment of adjacency information is based on the spatial and positional relationships of the tiles. To facilitate the computations of the crack removal algorithm, we define a marker called "Dirty" for the adjacency information of each edge and corner of every tile. Dirty has two possible states: active or

sleeping. The specific procedure is given in the following subsection.

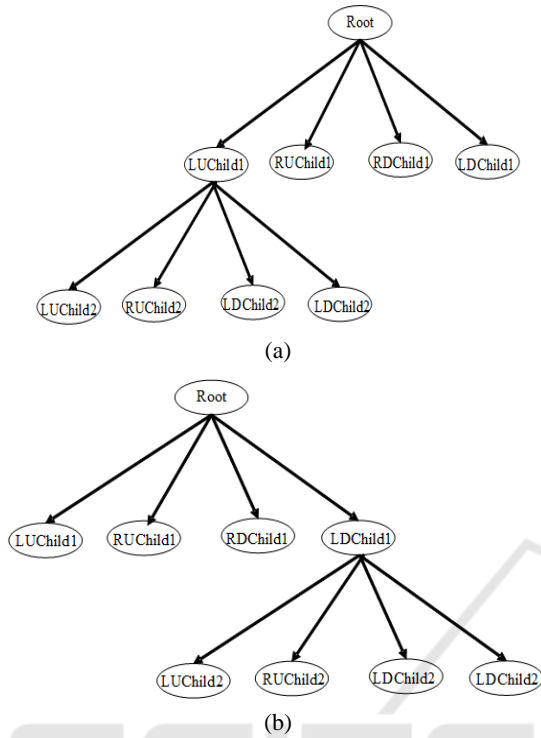


Figure 5: An illustration of a terrain quadtree being updated: (a) View located at the upper-left part of the terrain and (b) View located at the bottom-left part of the terrain.

3.2.1 The Processing of Adjacency Information for Split Leaf Nodes

The location of a split leaf node relative to its "parent" tile is determined, and the adjacency information of the former is then acquired using its location and spatial/positional relationships. The determination of the corner and edge neighbors of a "child" tile located at the upper-left corner of a "parent" tile (LUChild) is described below.

(1) The determination of edge neighbors and their states

Since the split leaf node is an upper left "child" tile, the tiles that neighbor the split leaf node on its right and bottom edges must belong to the same "parent" and have the same level of resolution. Hence, the "Dirty" crack removal markers of the following edges are set to the sleeping state: the right and bottom edges of the current tile, the left edge of the right-edge neighbor, and the upper edge of the bottom-edge neighbor. As the left and upper-edge neighbors have different "parents" than the current tile, the next step is to find the "parents" of the left

and upper edge neighbors of the current and to subsequently perform calculations for the left and upper-edge neighbors of the current tile. The "Dirty" crack removal markers of the edges associated with all the previously mentioned tiles are then set to the active state.

(2) Determination of corner neighbors and their states

As before (i.e., during the determination of edge neighbors and their states), the bottom-right corner neighbor of the upper-left corner "child" tile has the same parent as the current tile and therefore the same level of resolution. Thus, the "Dirty" crack removal markers of the bottom-right corner of the current tile and the upper-right corner of the bottom-right corner neighbor are set to the sleeping state. Since the upper left, upper right, and bottom left corner neighbors belong to different "parents" than the current tile, the next step is to search for the parents of the upper-left, upper-right and bottom-left corner neighbors of the current tile. The corner neighbors of the current node are then identified, and the "Dirty" crack removal markers of the corners associated with the current tile are set to the active state.

3.2.2 The Processing of Adjacency Information for Merged Leaf Nodes

Since four "children" are merged to form a "parent", it is necessary to update the adjacency information of the neighbors of these "children" in sequential fashion. Again, the "child" tile in the upper-left corner (LUChild) is used as an example to explain this process.

(1) The determination of edge neighbors and their states

The adjacency information of the right-edge and bottom-edge neighbors does not require further processing because these neighbors have the same parent as the current LUChild tile and because these three tiles are also simultaneously merged. If the left-edge (LN) and upper-edge (UN) neighbors have the same LoD as the LUChild tile, the adjacency information of the LN and UN tiles will change after the 4 "children" tiles have been merged. The right-edge neighbor of LN and the upper-edge neighbor of UN are set as the parent of LUChild. If LN and UN have "children" tiles, the adjacency information of their associated edges will then need to be recursively updated. The "Dirty" markers of the corresponding edges are also simultaneously set to the active state.

(2) The determination of corner neighbors and their states

As before, the adjacency information of the bottom-right corner neighbor is not processed since it has the same "parent" as the current tile (LUChild). If the upper-left corner neighbor (LUN) has the same LoD as LUChild, the bottom-right corner neighbor of LUN is then designated the "parent" of LUChild. If LUN has any "children", the adjacency information of the relevant corners then needs to be recursively updated. If an upper-right corner neighbor (RUN) or bottom-left corner neighbor (LDN) exists and has the same LoD as LUChild, the corner adjacencies related to these tiles must be set to null since they are not spatially adjacent to the corners of the "parent" of LUChild (like the O and UN2 tiles in Fig. 4). Similarly, if RUN and LDN have children, their corner adjacencies also need to be recursively updated.

3.3 The Removal of Cracks with Large Differences in Lod

To satisfy the requirements for the real-time rendering of massive terrain data, terrain frustum culling is used to perform a preliminary investigation of the range of tiles that require crack removal when the terrain renders and quadtrees of each frame are being constructed. The adjacent tiles and "Dirty" state of the newly added leaf nodes are determined; the nodes that have an active "Dirty" state may contain cracks, and these are stored in the crack repair set (CrackTileVector). After the preliminary investigation is complete, crack removal without LoD difference constraints is performed on the tiles of CrackTileVector.

Our crack removal algorithm without LoD difference constraints can be summarized as follows. Since terrain cracks can only occur at tile boundaries, the (four) edges and corners of some given tile are sequentially processed, and linear interpolation is used to ensure that the node elevations of the tile that is being processed are consistent with the node elevations of the adjacent tiles (which may have different LoDs). The steps in processing the left edge of a tile are used as an example to explain the specific processes of the proposed algorithm.

Step 1: Investigate the left-edge neighbor (a leaf node) of the current tile using dynamically updated tile adjacency information.

If the current node is N, the adjacency array of the left neighbor of N is Lvec() (the left-edge neighbor can exist in various configurations, as shown in Figs. 6(a), 6(b) and 6(c); nevertheless, the processing procedure is the same in each case). To find the left-

edge neighbor of N in a 3D terrain scene, each member of the Lvec(array) is checked for "children". If a member has "children", the upper-right and bottom-right "children" of this member (LChild1 and LChild2, respectively) are assigned to the current node (N) and treated as the left-edge neighbor of N. LChild1 and LChild2 are then recursively processed using these steps until a leaf node is reached and recorded in the neighbor array, LYvec[]. After the left-edge neighbor of N has been configured, the right-edge neighbor of the left-edge neighbor is simultaneously designated N.

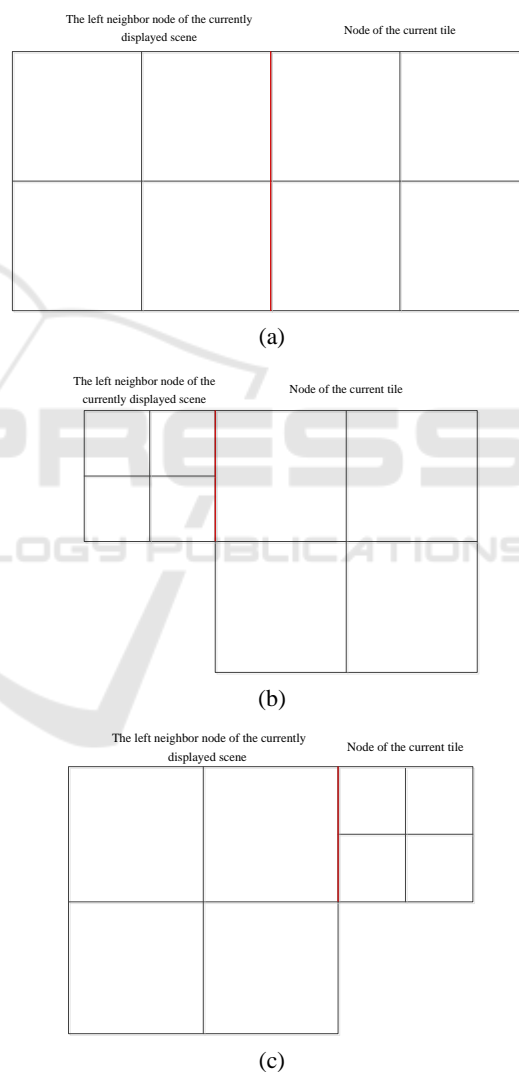


Figure 6: Possible configurations for the left-edge neighbor of a tile: (a) N and L have the same LoD, (b) N has a greater LoD than L and (c) N has a lower LoD than L.

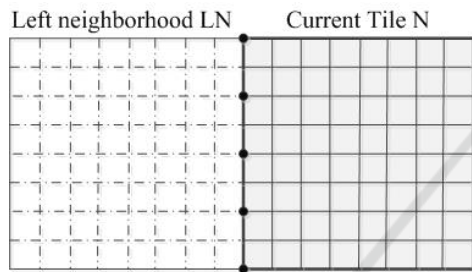
Step 2: For the array of left-edge neighbors (LYvec[]), perform the crack removal operation.

If there is only one node in $LYvec[]$, the left-edge neighbor and N then have the same LoD, and the vertex relations between the tiles have a strict one-to-one correspondence, as shown in Fig. 7(a). In this case, every vertex on the inter-tile boundary can be directly traversed to determine whether the vertices have the same elevation. If the elevations are not equal, the elevation of N is used as a reference, and the elevation values of the vertices are assigned to the corresponding vertices of the corresponding neighbors. If $LYvec[]$ only has 2 nodes and the LoDs of N and its neighbor are different by 1, the relationship between the boundary vertices of these tiles is then described by Fig. 7(b). Additionally, in this case, the length of two neighboring grids is exactly the length of a single N grid. Equidistant linear interpola-

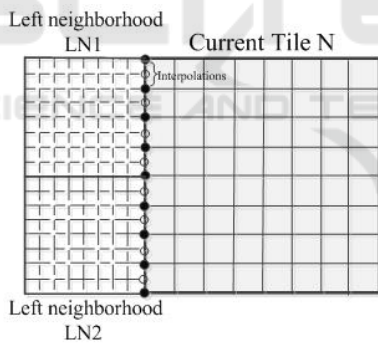
tion is then performed on the vertices of N to obtain the midpoint elevations between each pair of vertices on the boundary of N ; these elevation values are then assigned to the neighboring vertices. If $LYvec$ has 4 nodes and the difference between the LODs of N and the neighbor node is n ($n > 1$), the relationship between vertices of these tiles is as shown in Fig. 7(c) ($n = 2$). This figure illustrates that the length of two grids in the adjacent tile is $1/n$ the length of a grid in N . The grid points of N that are closest to the neighboring tile are then calculated, and the grid edges of N are divided in half to form $2n$ nodes. The linear interpolation algorithm is used to calculate the elevations of every node, which are then assigned to the neighboring vertices.

Since the vertex normals of the boundary mesh vertices must be recalculated, the “Dirty” markers of vector normals corresponding to vertices that still require crack removal are set to the active state.

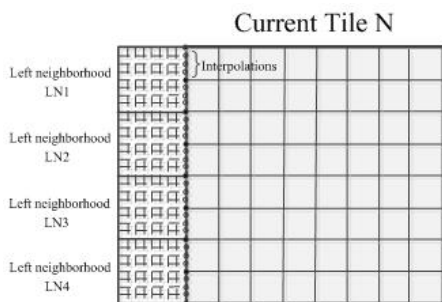
The proposed crack removal algorithm can be used without any constraints regarding the difference in boundary LoD between adjacent nodes. In addition, our method does not require the rendering of additional terrain patches, which helps to preserve actual changes in terrain elevation.



(a)



(b)



(c)

Figure 7: Possible configurations for the left-edge neighbor of a tile: (a)Same LoD, (b)Difference of 1 in LoD and (c)Difference of 2 in LoD.

3.4 The Updating of Vertex Normals in Boundary Areas

Lighting discontinuities may occur at mesh boundaries after the elevations of vertices at terrain cracks have been adjusted (Han et al, 2012). After the terrain cracks have been removed, the vertex normals of the boundary vertices that participated in the crack removal operation must be recalculated and re-evaluated. This process can be described as follows.

Step 1: CrackTileVector is sequentially traversed, and all the vertices on the four edges of each tile are processed to determine whether the “Dirty” marker of the vertex normal is set to the active state. If the “Dirty” marker is active, proceed to Step 2; otherwise, continue to the next vertex.

Step 2: Investigate the 8 vertices that are connected to this vertex by a triangular mesh, e.g., the 8 vertices around A in Fig. 8. If any of these vertices are missing, proceed to Step 3 to pad the vertices; otherwise, proceed directly to Step 4.

Step 3: Vertex padding. Like the crack removal algorithm, the first step in the padding process is to determine the LoD difference between the current tile and an adjacent tile. An analogous subdivision is performed via linear interpolation of the grids of the

tile with the lower LoD to generate a corresponding set of vertices in the former tile. Fig. 9 shows that the grids around the boundary of terrain block 1 should be subdivided, so that a vertex (b) can be identified on the right side of boundary point A to participate in the construction of a triangular mesh.

Step 4: Using the current vertex as the center, the normal components of each of the 8 directions from the current vertex are sequentially calculated. These components are then summed and normalized. Finally, the vertex normals of the current vertex are evaluated according to the results of these calculations.

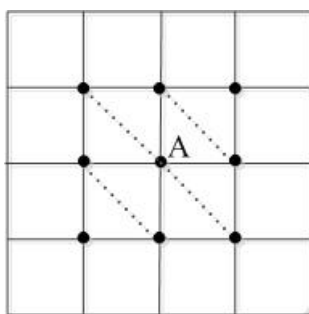


Figure 8: The vertices associated with point A.

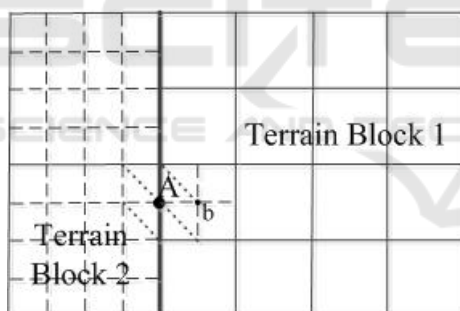


Figure 9: Analogous subdivision of boundary grids.

4 EXPERIMENTS AND ANALYSIS OF RESULTS

4.1 Experimental Data and Environment

The proposed terrain crack removal algorithm was embedded in the NewMap software platform developed by the Chinese Academy of Surveying and Mapping. The effectiveness of the method was then tested using the terrain data from a typical mountainous region in Sichuan Province. The elevation data were obtained from the Shuttle Radar Topography Mission (SRTM), with a coordinate range of (97.5° ~108.5° E, 26.2° ~34.1° N); the horizontal and vertical resolutions of the data were 90 m and 0.1 m, respectively. The image data were derived from the terrestrial remote sensing data from Landsat. The multiresolution elevation and image quadtree pyramids were constructed using NewMap TerrainPublish software, and the sizes of these pyramids were 15.76 GB and 63.34 GB, respectively. The hardware environment of this experiment was a PC equipped with a 2.60 GHz Pentium Dual Core E5300 CPU, 1.96 GB of internal storage, and a Nvidia GeForce 6800 graphics card.

4.2 Results and Analysis

4.2.1 Validating the Reliability of the Proposed Method

The proposed method was compared to the elevation adjustment-based crack removal method (i.e., the conventional method) to validate the reliability of our method. A random region was selected from the experimental data to compare the effectiveness of these methods in removing terrain cracks. The results of this experiment are shown in Table 1.

Table 1: Comparison of crack removal effectiveness.

	Total number of tiles	Number of terrain cracks					Rate of terrain crack removal
		LoD difference of 1	LoD difference of 2	LoD difference of 3	LoD difference of 4	Total number of cracks	
		2057	1080	384	64	3585	
Conventional method	17072	2057	-	-	-	2057	57.38%
Our method		2057	1080	384	64	3585	100%

Table 1 shows that there are large differences in LoD around the boundaries where terrain cracks occur. Terrain cracks with an LoD difference of 1 account for 57.38% of the total number of terrain cracks in the experimental area. The conventional method successfully eliminates all terrain cracks with an LoD difference of 1 but is unable to process terrain cracks with LoD differences greater than 1. Our method is able to completely eliminate all terrain cracks with LoD differences of 1 and terrain cracks with LoD differences greater than 1. Specifically, a terrain crack removal rate of 100% was achieved in this area using the proposed method. Figs. 10, 11 and 12 illustrate the effectiveness of the aforementioned methods in removing terrain cracks with LoD differences of 1, 2 and greater than 2, respectively.

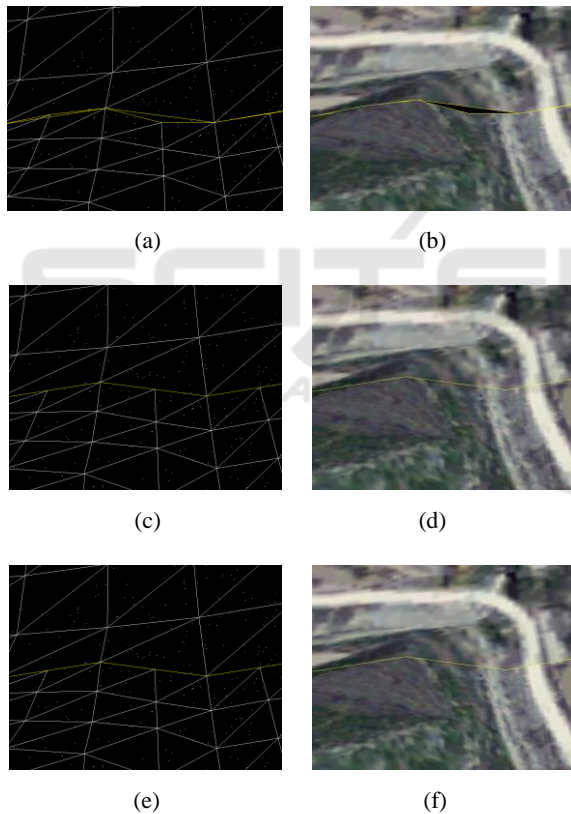


Figure 10: Comparison of our method and the conventional method for the removal of terrain cracks with an LoD difference of 1:(a)Terrain crack with an LoD difference of 1, (b)Visualization of the terrain crack, (c)Results of crack removal using the conventional method, (d)Results of crack removal using the conventional method, (e)Results of crack removal using our method and (f)Visualized result of crack removal using our method.

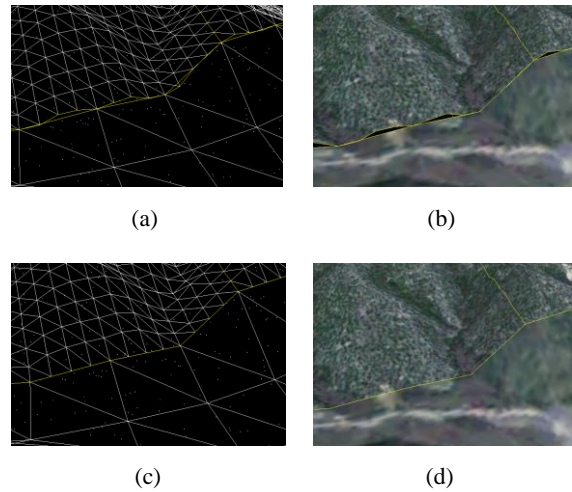


Figure 11: The effectiveness of our method in removing terrain cracks with an LoD difference of 2 : (a)Terrain cracks with an LoD difference of 2, (b)Visualization of terrain cracks, (c)Results of terrain crack removal using our method and (d)Visualized result of terrain crack removal using our method.

Figs. 10 and 11 clearly show that both the aforementioned methods can effectively eliminate terrain cracks that have an LoD difference of 1, and the proposed method is also suitable for removing terrain cracks that have LoD differences of 2, the complex terrain in the studied region is accurately reproduced by the processed terrain structures.

4.2.2 Validation of Lighting Continuity

By changing the rules applied for tile splitting, the tiles that are rendered in a scene will have the same LoD, which ensures that cracks cannot occur throughout the entirety of the terrain scene. In this case, the lighting of the meshes around tile boundaries is continuous, and this is referred to as the theoretical reference value. However, under normal tile splitting rules, the tiles that are rendered in a scene can have different LoDs, and these are the actual values of the vertex normals (lighting) after the crack removal process has been implemented. A comparison was made between the vertex normals calculated by our method and the conventional method for the tile boundaries of a terrain block to inspect the continuity of the lighting values in each case. The theoretical values and actual (post-crack removal) values of the vertex normals are shown in Table 2.

Table 2: Comparison of vertex normal at tile boundaries.

Vertex number	Theoretical value (X, Y, Z)	Vertex normals of the conventional method (X, Y, Z)	Vertex normals of our method (X, Y, Z)
1	(0.630410,0.279561,0.724174)	(0.630410,0.279561,0.724174)	(0.630410,0.279561,0.724174)
2	(0.623360,0.294948,0.724174)	(0.724351,0.134632,0.676158)	(0.623450,0.294758,0.724174)
3	(0.615934,0.310157,0.724174)	(0.615934,0.310157,0.724174)	(0.615934,0.310157,0.724174)
4	(0.608136,0.325179,0.724174)	(0.649363,0.623852,0.434898)	(0.608129,0.325194,0.724174)
5	(0.599973,0.340006,0.724174)	(0.599973,0.340006,0.724174)	(0.599973,0.340006,0.724174)
6	(0.591448,0.354628,0.724174)	(0.639341,0.398756,0.657447)	(0.591449,0.354630,0.724172)
7	(0.582567,0.369035,0.724174)	(0.582567,0.369035,0.724174)	(0.582567,0.369035,0.724174)
8	(0.563758,0.397176,0.724174)	(0.737288,0.423349,0.526481)	(0.563761,0.397176,0.724172)
9	(0.573335,0.383221,0.724174)	(0.573335,0.383221,0.724174)	(0.573335,0.383221,0.724174)
10	(0.543590,0.424360,0.724174)	(0.415249,0.628213,0.657964)	(0.543588,0.424363,0.724174)
11	(0.553841,0.410892,0.724174)	(0.553841,0.410892,0.724174)	(0.553841,0.410892,0.724174)
12	(0.533012,0.437573,0.724174)	(0.743681,0.577819,0.336250)	(0.533012,0.437573,0.724174)
13	(0.522113,0.450522,0.724174)	(0.522113,0.450522,0.724174)	(0.522113,0.450522,0.724174)
14	(0.499378,0.475598,0.724174)	(0.657243,0.261486,0.706864)	(0.499381,0.475595,0.724174)
15	(0.510899,0.463199,0.724174)	(0.510899,0.463199,0.724174)	(0.510899,0.463199,0.724174)

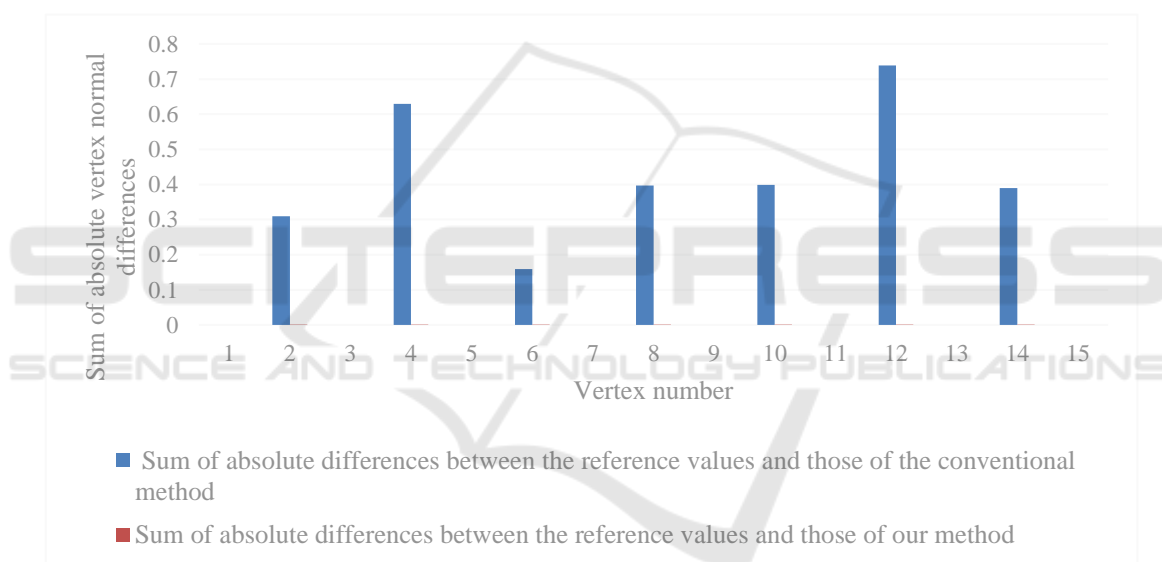


Figure 12: Comparison between the boundary vertex normals calculated by our method and the conventional method.

The red underlines in Table 2 serve to highlight differences between the theoretical and actual values of the vertex normals. The X, Y and Z components of the vertex normals that were calculated by the conventional method and our method were subtracted from the reference values, and the absolute values of these results were then summed to produce the bar chart shown in Fig. 12. This figure shows that the vertex normals calculated by our method for all 15 vertices (which are tile boundary vertices) are essentially identical to the theoretical values. Notably, only minor differences were observed at the 5th decimal place and beyond, which are negligible in the calculation of terrain tile lighting. However, there are significant differences between the vertex normals

calculated by the conventional method and the theoretical values, particularly for vertices 2, 4, 6, 8, 10, 12 and 14. These differences will lead to discontinuities in the lighting of tile boundaries.

4.2.3 Efficiency Validation

The efficiency of our method was validated by setting the view to roam around the experimental area for 20 minutes. During this time, the total number of tiles, number of cracks and time consumed by crack removal in every frame of the terrain rendering process was randomly sampled at 12 instants. The results are shown in Table 3.

Table 3: Crack removal statistics.

Time point (s)	Frames rendered	Total number of tiles	Total number of cracked tiles	Proportion of cracked tiles	Time consumption of our method (ms)	Time consumption of the conventional method (ms)
8.13	1025	244	30	12.30%	0.670	7.425
24.70	3458	273	8	2.93%	0.104	8.105
50.35	6643	396	16	4.04%	0.672	9.362
64.13	8721	355	21	5.92%	1.302	7.853
86.03	12474	473	13	2.75%	0.314	9.537
113.73	16149	440	19	4.32%	0.531	9.046
258.79	36231	492	26	5.28%	2.623	9.951
275.1	41264	212	22	10.38%	1.451	6.433
419.21	54498	516	24	4.65%	1.534	9.427
507.17	66439	460	28	6.09%	2.352	8.854
790.74	104378	543	49	9.02%	2.858	9.364
898.84	119546	316	31	9.81%	1.692	7.223

Table 3 shows that the proposed method requires less computational time than the conventional method because our method only computes the “parent” nodes obtained from newly split or merged leaf nodes during terrain crack removal; hence, only the tiles that correspond to terrain cracks are processed. During crack removal with the conventional elevation adjustment-based method, the entirety of the terrain quadtree must be traversed; therefore, all the tiles must be processed when this method is used. This approach consumes more computational time, and the average processing time of the conventional method is approximately 8 times that of our method.

5 CONCLUSIONS AND DISCUSSION

In this work, we have proposed a terrain crack removal method that is able to handle large differences in boundary LoD. This method fully exploits the features of quadtree structures and the implicit adjacency relationships of parent and child nodes. Additionally, terrain crack removal and the updating of boundary vertex normals occur in real time. With this method, the elimination of terrain cracks will no longer be limited by differences in boundary LoD. The following conclusions were drawn from the validations and comparative analyses that were performed using terrain data from a typical mountainous region in Sichuan Province.

(1) Our method is applicable at boundaries where the difference in LoD is equal to 1 and complex terrain areas where the LoD difference between adjacent tiles is greater than 1.

(2) The continuity of terrain lighting is ensured by our method through the recalculation and re-evaluation of boundary vertex normals after the crack removal process, thereby overcoming the lighting discontinuities that hinder the use of the conventional crack removal method.

(3) The efficiency of our method is, on average, eight times greater than that of the conventional method because the proposed method does not traverse the entirety of the terrain quadtree during crack removal, which saves a substantial quantity of computational time.

The method that is proposed in this work is suitable for terrain rendering based on quadtree structures. However, further research must be performed to investigate the suitability of the method for other terrain mesh models, such as triangular meshes and binary tree models.

ACKNOWLEDGEMENTS

This research was funded by a project supported by the National Key Research and Development Program of China (Grant No. 2016YFF0201305) and National Natural Science Foundation of China (Grant No. 41871375).

REFERENCES

- Bulatov D, Häufel G, Meidow J, et al. 2014. Context-based automatic reconstruction and texturing of 3D urban terrain for quick-response tasks. *Isprs Journal of Photogrammetry & Remote Sensing*, 93(7):157-170.
- Feng W W, Kim B U, Yu Y, et al. 2010. Feature-preserving triangular geometry images for level-of-detail representation of static and skinned meshes. *Acm Transactions on Graphics*, 29(2):11-22.
- Fu W, Ge Z H, Li W H. 2012. A terrain rendering method with dynamic error metric for flight simulation. *Journal of Jilin University (Science Edition)*, 50(6): 1175-1178.
- Han L T, Kong Q L, Dai H L, et al. 2012. Optimization of normal calculation of regular grid terrain based on OpenGL. *Science of Surveying and Mapping*, 37(5):17-19.
- Han M, Tang S T, Li Y. 2008. Real-time visualization algorithm of large-scale terrain. *Computer Engineering*, 34(13):270-272.
- Ke X L, Zeng J. 2005. Dynamic rendering for LOD virtual terrain using quadtree. *Bulletin of Surveying and Mapping*, (6):10-13.
- Li Q, Dai S L, Zhao Y J, et al. 2013. A block LOD real-time rendering algorithm for large scale terrain. *Journal of Computer-Aided Design & Computer Graphics*, 25(5):000708-713.
- Liu Y, Guan A D, Li J. 2010. A model for massive 3D terrain simplification based on data block partition and quad-tree. *Acta Geodaetica et Cartographica Sinica*, 39(4):410-415.
- Nie J L, Liu S, Guo D L, et al. 2013. GPU-accelerated fast rendering method for multi-resolution geometry image. *Journal of Computer-Aided Design & Computer Graphics*, 25(1):101-109.
- P Lindstrom, V Pascucci. 2001. Visualization of Large Terrains Made Easy. *Proceedings of IEEE Visualization*. 363-370.
- Wan M, Liang X, Zhang F M. 2015. Improved crack removing algorithm for quad-tree terrain rendering. *Journal of System Simulation*, 27(7):1520-1525.
- Wang D C, Wan W G, Tang J Z, et al. 2007. Preprocessing LOD algorithm for large scale terrain based on restricted quadtrees. *Computer Engineering and Applications*, 43(24):107-109.
- WIESEMANN T, SCHIEFE LE J, KUBBAT W. 2005. Multi-resolution Terrain Depiction on an Embedded 2D/3D Synthetic Vision System. *Aerospace Science and Technology*, 9 (6):517-524.
- Xu M Z. 2005. Research on Real-Time Rendering for Large Scale Terrain. *Geomatics and Information Science of Wuhan University*, 30(5):392-395.
- Yang Y, Wang C, Gao Y, et al. 2014. Large Scale Terrain Real-Time Rendering on GPU Using Double Layers Tile Quad Tree and Cuboids Bounding Error Metric. *Open Automation & Control Systems Journal*, 2014, 6(1):1378-1388.
- Yin Y, Chen G J, Wu W. 2006. An algorithm of avoiding crack for rendering parting terrain. *Journal of Computer-Aided Design & Computer Graphics*, 18(10):1557-1562.
- Zhao X S, Fan D Q, Wang J J, et al. 2012. Seamless expression of the global multi-resolution DEMs based on degenerate quadtree grids. *Acta Geodaetica et Cartographica Sinica*, 41(6):918-925.
- Zhao Y B, Shi J Y. 2002. A fast algorithm for large scale terrain walkthrough. *Computer-Aided Design & Computer Graphics*, 14(7):624-628.
- Zheng X, Liu W, Lu C L, et al. 2013. Real-time dynamic storing and rendering of massive terrain with GPU. *Journal of Computer-Aided Design & Computer Graphics*, 25(8):1146-1152.